



Microstructure, thermal, and mechanical properties of friction stir welded 6061 aluminum alloy with 10% SiCp reinforcement

H. I. Dawood^{1*}, Kassim Kadhim Hameed Alshemary¹, Abbas Khalaf Mohammad¹,
Nawras Shareef Sabeeh²

¹Department of Chemical Engineering, College of Engineering, University of AL-Qadisiyah, AL-Qadisiyah, IRAQ

²Department of Mechanical Engineering, College of Engineering, University of AL-Qadisiyah, AL-Qadisiyah, IRAQ



CrossMark

Abstract

After 10 vol. % SiC particles from the welding volume were inserted into the joint line, the mechanical properties of friction stir-welded joints were assessed. During the Friction Stir Welding (FSW) process, three different rotational speeds (1300, 1750, and 2000 rpm) were used. Field Emission Scanning Electron Microscopy (FESEM) was used to examine the microstructure across the Stir Zone (SZ), revealing a banded structure between the particle-rich and particle-free portions of the SiCp. When the joint was constructed at 1750 rpm, it displayed better mechanical properties. Because of the presence of SiCp, the Ultimate Tensile Strength (UTS) was enriched by 79.6% at 1750 rpm. Because of the pinning effect and larger nucleation sites caused by the SiC powder, this strength significantly increased. Furthermore, the hardened particle powder cracked the initial grains. When compared to the SiC-free sample, the SiC-rich sample had higher ductility at 1750 rpm. Finally, the fracture surface showed a good agreement with the equivalent ductility marks.

Keywords: Friction stir welding; 6061 aluminum alloy; Aluminum matrix SiC_p; Microstructure; Mechanical properties.

1. Introduction

Welding defects in aluminum alloys, such as porosity and solidification fractures, degrade weld quality and joint properties [1]. Defective welds are obtained when conventional fusion welding methods are employed to join aluminum matrix composites. Fusion welding during solidification is produced unwanted chemical interactions between the enhanced and molten matrix metals [2, 3]. On the contrary, during FSW the main material is not dissolved and recasted. FSW is a solid-state method for connecting different materials [1, 4-6] and eliminates the aforementioned problems. The FSW process was firstly known at The Welding Institute, UK in 1991 [7]. This welding method generates an asymmetric microstructure that is represented by the advancing and retreating sides. If the rotary tool path is in the same welding direction, it is indicated to the advancing side; otherwise, it is indicated to the retreating side. Heat transfer, material flow, and weld

properties can all be affected by differences in features on both sides [8].

Many researches have been carried out to investigate the influence of the FSW process parameters on FSW of aluminum alloys [4, 6, 9-17]. In the reported works the FSW process parameters namely tool rotational speed and welding speed has been varied to examine its influences on the microstructure, tensile strength, and microhardness on the weld joint. At various rotational speeds Kim et al. [18], studied the FSW of aluminum die casting alloy. The size of the SiCp at the bottom of the SZ was found to be less than at other places of the SZ for any tool rotating speed. In all SZ positions, the influence of rotating speed on SiCp size was not significant. Uzun and Huseyin [19] investigated the FSW of SiCp reinforced 2124 aluminum alloy matrix using Scanning Electron Microscopy (SEM). In the SZ, some of voids or pores formation was observed at the coarse SiCp / matrix interface. This was attributed to the composite's SZ high stirring rates. The fracture of certain coarse SiCp

*Corresponding author e-mail: hasan.dawwood@qu.edu.iq

Receive Date: 12 December 2021, Revise Date: 17 December 2021, Accept Date: 20 December 2021

DOI: 10.21608/EJCHEM.2021.110858.5053

©2022 National Information and Documentation Center (NIDOC)

in the SZ was also observed by SEM. The above events were described by the researchers as a result of excessive stirring of SiC_p with matrix aluminum alloys in the SZ. Storjohann et al [20] have investigated the microstructure of the friction stir welded alloys 2124 aluminum/ SiC_p and 6061 aluminum/Al₂O₃ alloys. In both cases, the enhanced particles are expected distributed uniformly and there was no indication that deleterious reactions have occurred in the SZ, which is consistent with earlier research in this field. Hardness measurements showed slight difference between the SZ regions and the parent metal in both the alloys. Storjohann et al [20] also interpreted how the FSW joining process has an influence on the orientation of the SiC_p reinforcements. It is found that preferred mechanical properties in the finished joint significantly dependent upon the post weld distribution of the enhanced particles.

Friction Stir Processing (FSP), which is an extension of FSW, was also utilized to create a surface composite of different-sized reinforcing particles [21, 22]. The effect of the number of passes on the particle distribution has been evaluated. Results show a direct correlation between the number of passes and improved particle distribution [23-26]. In addition, the mechanical properties of the fabricated composites were investigated based on the influence the different ratios of rotational speeds to travelling speeds [27, 28]. Barmouz et al. [21] observed that increasing the rotational speed leads to reduced grain size in the SZ when Cu was fabricated with SiC_p -reinforced. They also discovered that the grain particle size of the synthesized composite layers is much less than that of the SiC_p-free sample. At 1120 rpm and 80 mm/min Dolatkah et al. [29] observed uniform SiC_p powder distribution in the FSP of 5052 aluminum alloy. Previous research has examined the

Table 1 Chemical compositions of 6061 aluminum alloy (in wt %) [32].

Element	Al	Si	Fe	Mg	Cu	Mn
%	97.57	0.525	0.339	1.062	0.120	0.080

impact of particle-reinforced between passes on microstructure and mechanical properties [29, 30]. Sun and Fujii [31] introduced SiC_p into 2-mm thick copper plates using FSW. A copper matrix composite was successfully formed within the SZ, according to the studies.

The FSW with reinforcement particles has been applied on several metals and alloys. From the above review, it is understood that many researchers performed investigations on FSW of metal–matrix composites to know the main welding parameters that affect flow behavior, metallurgical and mechanical properties. Lack of information was reported so far on the effect of process parameters on metallurgical and mechanical properties of friction stir welded 6061 aluminum alloy / SiC_p metal–matrix composites.

The aim of the current study is to investigate the effects of SiC_p and tool rotatory speed on the microstructure, tensile strength, fracture surface, microhardness and thermal effects of friction stir-welded joints of 6061 aluminum alloy. In addition, this work involved estimating the optimal operating condition of the FSW process. Four separate specimens represented the relationship between three different input parameters of rotational speeds and each one of the considered characteristics of the SZ.

2. Experimental procedures

The chemical composition of the 4 mm thick 6061 aluminum alloy plate used in this study is shown in Table 1. Fig.1a shows the FESEM magnified micrograph of the as-received SiC_p. As shown in Fig. 1b, the FSW tool was machined from medium carbon steel and heat-treated to 60 HRC. A threaded taper pin with a diameter of 2 mm, a shoulder diameter of 10 mm, and a pin height of 3.7 mm was inscribed in a circle.

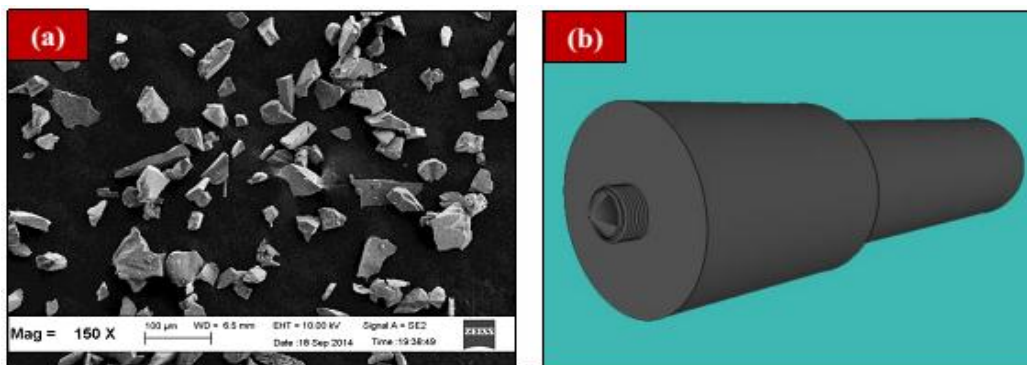


Fig. 1: (a) FESEM micrograph of SiC_p and (b) the stir weld tool.

A cutting band saw machine was used to cut the aluminum plate into 210 mm x 200 mm strips: (Model: UE-712A). Afterwards, a built fixture pressed a 10% volume of SiCP from the welding volume between two strips (Fig. 2). A tool shoulder with no pins was chosen to submerge the powder before the FSW process in order to fix the SiCP across the joint line without any dissipation during the welding process. After that, three different rotational speeds (1300, 1750, and 2000 rpm) as well as a travel speed of 40 mm/min were tested. A single-pass FSW was performed in each case. Table 2 lists the specimen data and processing conditions. In this investigation, the optimal rotational speed was found to be 1750 rpm, which matches to Hasan et al. [32]. Furthermore, the enhanced particles at this parameter have a consistent uniform distribution [particle-rich regions] across the interface section that connects two pieces of 6061 aluminum alloy. As a result, the specimen that was friction stir welded at 1750 rpm had the best mechanical properties. Furthermore, FSW was performed at a best processing speed (1750

rpm) but the specimen without SiCP performed to understand the impact of particles on the joint's microstructure and mechanical properties.

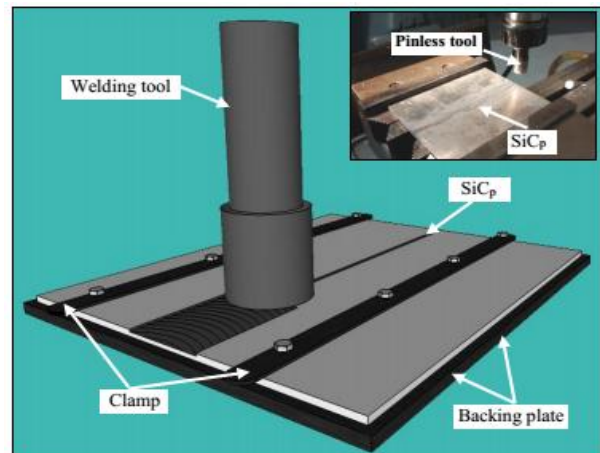


Fig. 2: Friction stir welding fixture.

Table 2 Review of the FSW joints properties.

Rotational speeds	1300 rpm	1750 rpm	2000 rpm	1750 rpm (without SiC _p)
Grain size (μm)	2.878	1.8	3.579	7.371
Percentage of elongation	5.4	5.8	5.6	4.8
Average microhardness value (Hv)	95	105	89	88
UTS (MPa)	197.538	283.158	164.797	151.035

During the FSW process, K-type grounded thermocouples with a diameter of 1 mm were attached to the workpiece surfaces at various positions close to the tool shoulder's boundary to measure the temperature around the joint line (Fig. 3). Prior to the preparation of the metallographic and tensile specimens, the upper surfaces of the FSW joints were machined to remove the marks left by the shoulder. The samples for metallographic examination were prepared for microstructural evaluation by cross-sectioning them perpendicular to the welding line direction. After that, the metallographic specimens were chemically etched for 15 minutes with 1% NaOH. The ASTM:E112-96 linear intercept method was used to determine the mean grain size [33]. The sub-sized tensile specimens were mechanically discharged and machined perpendicular to the welding direction according to ASTM: E8/E8M-11, B557: ETD 2013. The fracture surface was studied using FESEM and Energy Dispersive X-ray (EDX) analysis. The elements were analyzed using an EDX in combination with FESEM. The SZs' microhardness was tested using a Vickers micro-hardness (Hv) tester with a 1 kgf load for 15 seconds.

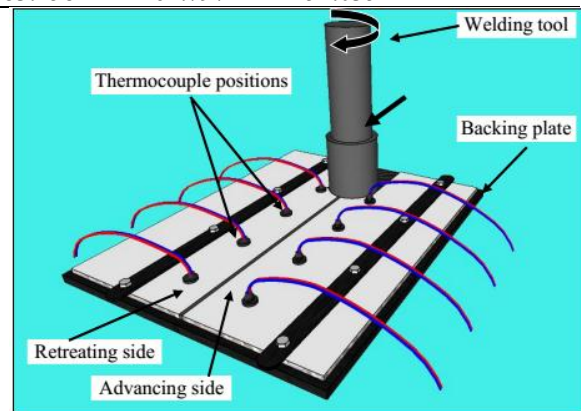


Fig 3: Friction stir welding process showing thermocouple positions.

1. Results and discussions

1.1. Microstructural investigation

Base Metal (BM), Heat-Affected Zone (HAZ), Thermo-Mechanically Affected Zone (TMAZ), and SZ are the four zones that form the FSW process [34]. Fig. 4a illustrates the microstructure of the sample in which NZ, TMAZ, and HAZ are distinguished in a clarified way. Fig. 4b shows the magnified microstructure at the interface between TMAZ and HAZ. Figs. 5(a and b) show the FESEM images obtained from the SZ of the joints welded with SiC_p reinforcements at 1300 rpm and

2000 rpm, respectively. The micrographs of the SZ of the joints fabricated with or missing SiC_p at 1750 rpm are shown in Figs. 6 (a and b) respectively.

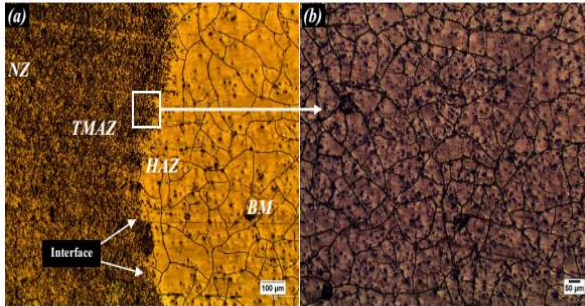


Fig. 4: (a) Major regions of friction stir weld and (b) magnified microstructure of the interface between TMAZ and HAZ.

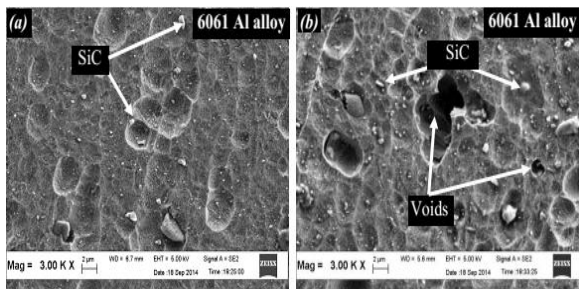


Fig. 5: FESEM images of the SZ welded with SiC_p at (a) 1300 and (b) 2000 rpm

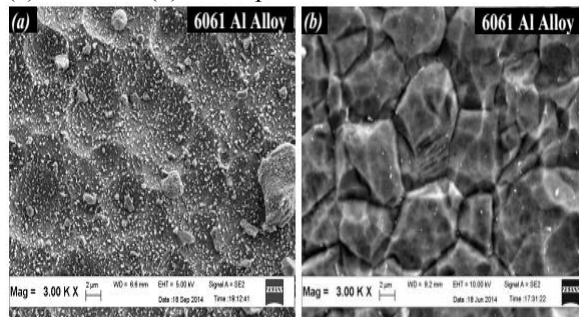


Fig. 6: FESEM images of the SZ welded at (a) 1750 rpm with particle-rich zones of SiC_p and (b) 1750 rpm without SiC_p.

When a material is exposed to intense plastic deformation at a high temperature during FSW, fine particles are produced. Dynamic recrystallization is the term for this phenomena. [35-37]. In the case of FSP without SiCP, the heat input is the most important component in determining particle size. However, the circumstances are different in the case of FSP with the presence of SiCP. [23]. Higher temperatures enhance the movement at the grain boundary [38]. Thus, a higher heat input along with increased rotational speed or decreased welding travelling speed hastens particle growth causing coarsens the recrystallized particles [27, 39, 40]. The SiC_p reinforcements could behave as barriers

adjacent to particle boundaries and grain growth impediment by limiting grain activities, this influence is known as pinning effect [37, 41]. The SiC_p reinforcements could break up the initial grains during plastic deformation. When grains are broken and a large number of low-angle disoriented grain boundaries are formed, more nucleation sites are produced [21]. During dynamic recrystallization, low-angle boundaries are converted to high-angle ones, resulting in the nucleation of new particles at discriminatory sites. In addition, when SiC_p exists, the nucleation sites for recrystallization increases [42].

It has been researched how to create discontinuous particle-rich and particle-free zones [31, 40, 43]. Particle-free zones within the SZ and the particle-rich banded structure of specimens fabricated at 1300 and 1750 rpm are shown in Figs. 5(a) and 6(a), respectively. Azizieh et al. [40] observed a similar structure in the friction stir-processed AZ31-Al₂O₃. The average value of the grains in the particle-rich regions in Fig. 6a was measured by linear intercept method and found less than that in the particle-free zones in Fig. 5a. (Table 2) Moreover, much finer grains were observed when the SiC_p was individually dispersed. Large grain sizes were observed at 1300 rpm, which proposes the key role of stirring effect in controlling the particle size. By contrast, finer grains were obtained at 1750 rpm. This phenomenon emphasis the vital effect of heat input factor to the stirring action of the pin. Grain growth was observed at 2000 rpm, which is due to the efficiency of heat input factor and stirring effect of the pin [18].

As aforementioned, the rotary speed of 1750 rpm in the present study was taken into account as the crucial processing parameter. The welding parameters in the FSW of the sample carried out at 1750 rpm with missing of SiC_p were maintained identical to the sample welded at 1750 rpm with particles enhancement. The aim of this action is to establish the influence of SiC_p reinforcements on the microstructure of SZ. In comparison to the sample friction stir welded at 1750 rpm without SiCP, particle size measurements revealed that grain refinement in the sample friction stir welded with SiCP was better. This is due to the thermal conductivity of SiCP, which dissipated high-heat flow and caused a rapid drop in temperature as compared to the synthesized joint with no particles reinforcement. High heat input is related with larger particle size of specimens welded without reinforcing particles. Sample friction stir welded at 1750 rpm with SiCP revealed a remarkable distribution of reinforcements; as a result, this specimen was designated as the optimal heat input specimen. However, for specimens welded at 1300 and 2000

rpm, which were considered as low and high-heat input specimens, respectively, a sharp gathering of SiC_p was observed in the advancing side. The perfect gathering of SiC_p and the excellent bonding with the aluminum matrix are depicted in Fig. 6a. Thus, it can be inferred that the smaller particle size of sample welded with SiC_p is due to the effects of reinforcement, namely, increased nucleation sites, broken primary grains, and suppression of grain boundary movement [42].

Fig. 7 describes the EDX peak obtained from the evaluated area at the SZ with a rotational speed of 1750 rpm and confirms the presence of SiC_p reinforcements. The homogeneous distribution of SiC_p is important and difficult to achieved, which can be enhanced by rising the number of passes [24-26, 29]. Improved dispersion uniformity leads to improved welded joint mechanical characteristics. Despite the fact that the effect of the number of passes on SiC_p distribution is not examined in this work, a verified degree of reinforcement collection is unavoidable, according to the literature [23].

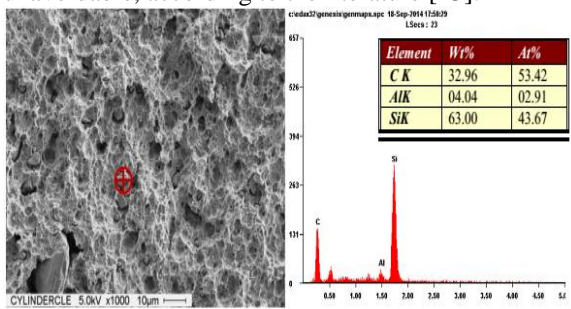


Fig. 7: EDX peak of SiC_p at the SZ welded at 1750 rpm.

3.2. Mechanical properties

3.2.1. Tensile properties

Tension tests reveal information about a material's strength and ductility when it is subjected to uniaxial tensile stresses. The information gathered could be valuable in material comparisons, alloy development, quality control, and design under specific circumstances. The subsized tensile tests of the specimens of FSW joints were cut perpendicular to the welding direction and performed at room temperature.

Many of microstructural factors like, dislocation density, grain size, and communication between the BM and the enhanced particles, control mechanical properties [21]. Figure 8 shows the tensile test results for all friction stir-welded joints. The results show that the specimens friction stir welded at tool rotational speed of 1750 rpm with and without SiC_p reinforcement demonstrated the greatest and the lowest UTS values, respectively. In addition, the UTS of 1750 rpm sample with SiC_p were higher than those of specimens conducted at 1300 and 2000 rpm with SiC_p reinforcement, but with significant

differences. The higher UTS of 1750 rpm specimen with SiC_p could be due to its fine particle size. According to Hall-Petch correlation, a drop in particle size leads to an improvement in the tensile properties [38]. The UTS of 1750 rpm specimen with SiC_p was enhanced by 79.6 % if compared with the BM relative to 1750 rpm specimen without SiC_p reinforcement (42.4 %) [20].

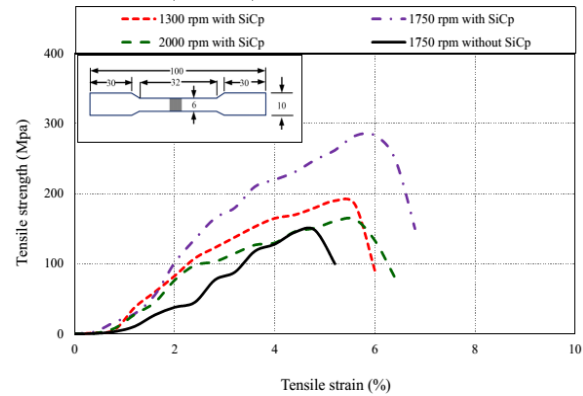


Fig. 8: Effects of using different rotational speeds with and without SiC_p reinforcement on the tensile strain-stress curves.

3.2.2. Fractography

FESEM micrographs of the tensile fracture surfaces of the specimens friction stir welded at 1300 and 2000 rpm are shown in Fig. 9. In those samples, a ductile fracture mode was discovered, emphasizing the considerably enhanced ductility (Figs. 9(a-d)). The FESEM micrographs of 1750 rpm specimens with and without SiC_p are depicted in Figs. 10(a-d); a cross-section of the fractured surface of the sample conducted at 1750 rpm with SiC_p reinforcement exhibits the characteristics of ductile fracture, while 1750 rpm specimen without SiC_p exhibited partial brittle and ductile fracture. However, 1750 rpm specimen with SiC_p was fractured from the border line of HAZ and BM zone, which confirms that the weld quality was enhanced. As a result, the site of the weld fracture represents the place of minimum microhardness.

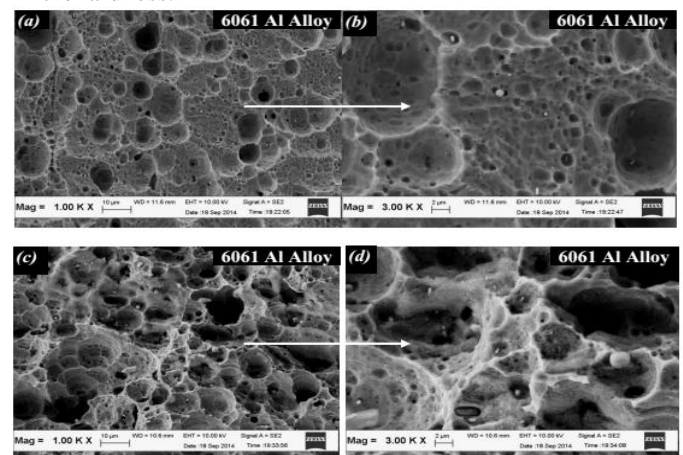


Fig. 9: FESEM micrographs of the tensile fracture surfaces of specimens welded at (a, b) 1300, (c, d) 2000 rpm, with the reinforcement of SiC_p.

1750 rpm specimen without reinforcement of SiC_p showed mainly brittle and ductile fracture surface mode as depicted in Figs. 10(c) and (d). This specimen was fractured from the limit of peak area between SZ and TMAZ. The fracture location for this tensile specimen was attributed to the two reasons. The first reason is due to the existing of some voids due to high heat input. The other reason is the TMAZ usually experienced deformation more likely than recrystallization. Accordingly, during tensile strength test, dislocation impact occurs more rapidly in the TMAZ than that in the BM. As a result, the applied stress is concentrated in this zone until fracture nucleation occurs [21].

Moreover, low and high heat input specimens (i.e. 1300 and 2000 rpm) were fractured from the hardly packed SiC_p region at TMAZ on advancing side. This result agrees well with Barmouz et al. [21] and Sun and Fujii [31]. Sun and Fujii reported that a one-pass manufactured copper joint containing SiCP was cracked in the region where SiCP had accumulated deeply [31].

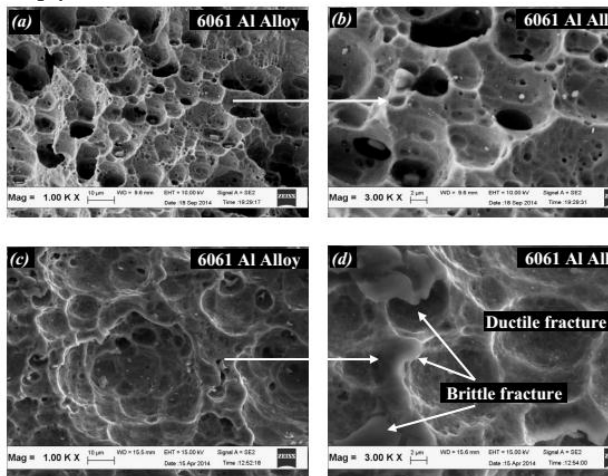


Fig. 10: FESEM micrographs of the tensile fracture surfaces of specimens welded at (a, b) 1750 rpm with SiC_p reinforcement, (c, d) 1750 rpm without the reinforcement of SiC_p.

3.2.3. Vickers Microhardness

The average value of microhardness of the as-received 6061 aluminum alloy after carrying out microhardness test was found about 94 Hv. The microhardness of a composite joint is closely associated with particle size, dislocation density, existence of the enhanced particles, and heat input. According to the Hall-Petch equation, smaller particles are accompanied with larger microhardness values [24].

$$H_v = H_0 + K_H d^{-1/2} \quad (1)$$

Where H_v is the hardness, H_0 and K_H are the appropriate constants associated with the hardness measurements, and d is the grain size. Dislocations generated from an imbalanced coefficient of thermal expansion of the matrix and enhancing phase result in greater microhardness [29]. Enhanced grains have double effects on microhardness because of the influence of the SiC_p on particle boundary pinning [24]. The microhardness of SZ is greater than that of BM is attributed to the strong bonding conduct between the dispersed SiC_p and the aluminum matrix composites. Although, the decreasing trend of microhardness may occur because of the annealing effect accompanied with heat input [28]. The behavior of the microhardness of the samples is depicted in Fig. 11. It could be noticed from this figure, the distribution of microhardness along the SZ are reduced. This occurrence appears from the mode of distribution of the powder reinforcement [31]. In this study, the average microhardness value was measured for use as a criterion, because microhardness distributions are not regular in the SZ due to the SiC reinforcement.

The comparative graph of average microhardness values is shown in Fig. 12. The maximum microhardness was obtained in sample friction stir welded at 1750 rpm with presence of SiC_p, which is attributed to the harsh distribution of the particles reinforcement. By contrast, the lower microhardness was observed in the same specimen welded at 1750 rpm but without reinforcement of SiC_p. Nevertheless of getting a lower and higher heat input, the microhardness of specimens welded at 1300 and 2000 rpm with SiC_p was lower than that of specimen welded at 1750 rpm with SiC_p reinforcement. This result is attributed to the major stirring effect of the pin and heat input factor at 1750 rpm with reinforcement of SiC_p. The proper stirring effect caused in more homogeneous particles distribution and consequently smaller particle size in sample friction welded at 1750 rpm with SiC_p relative to other specimens. The microhardness values of specimens conducted at 1300, 1750 and 2000 rpm (without particles reinforcement) indicate inferior microhardness compared to the same specimens conducted with SiC_p powder, because of the larger grain sizes and suggesting that in the absence of pinning effects.

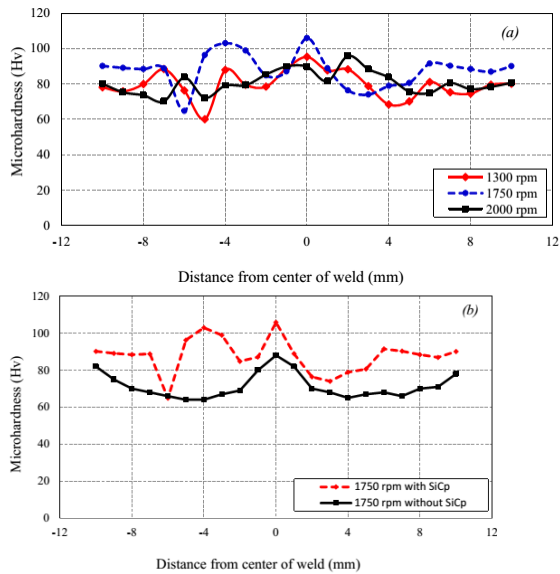


Fig. 11: Micro-indentation hardness behavior of specimens welded at (a) 1300, 1750, and 2000 rpm with SiC_p and (b) 1750 rpm with and without SiC_p.

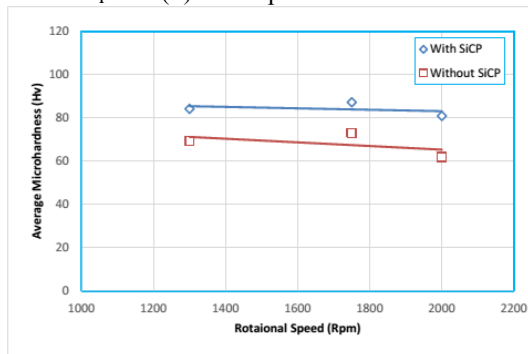


Fig. 12: Comparative diagram of average micro-indentation hardness.

Figure 13 shows the findings on the connection between Vickers microhardness and particle size in the SZ at various rotational speeds with and without SiC_p reinforcement. In this graph, Vickers microhardness is plotted against the reciprocal of the square root of the SZ particle size using the Hall-Petch equation (Eq. 1). The microhardness is roughly proportional to $d^{-1/2}$, as shown in the figure. Consequently, as the particle size decreases, the microhardness values increase.

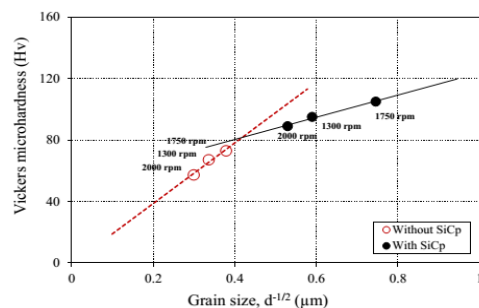


Fig. 13: Relation between Vickers micro-indentation hardness and average $d^{-1/2}$ of the SZ under various

rotational speeds with and without reinforcement of SiC_p.

3.3. Variation in temperature with respect to rotational speeds

The temperature during the FSW process of 6061 aluminum alloy was measured using a 1 mm K-type thermocouple with a digital screen and preset along the weld line (approximately 1 mm from the periphery of the tool shoulder) by using a thermal transfer paste. FSW generates temperature gradients close to the weld joint because of the frictional process between welding tool and workpieces. The temperature in the friction interface quickly increased because of the integration of friction and plastic work. The results gained in the experimental work of the temperature distributions on the top surface of the workpieces and align to the boundary of tool shoulder were measured for different rotational speeds. Fig. 14 shows that the rotational speed increased as the frictional temperature increased. Noticeably, the joints friction-stir weld at three different rotational speed without SiC_p had higher surface temperature compared with the similar joints friction-stir weld with particles reinforcement. As mentioned previously, this result is caused by the thermal conductivity of SiC_p if compared to the joints conducted without grain reinforcement.

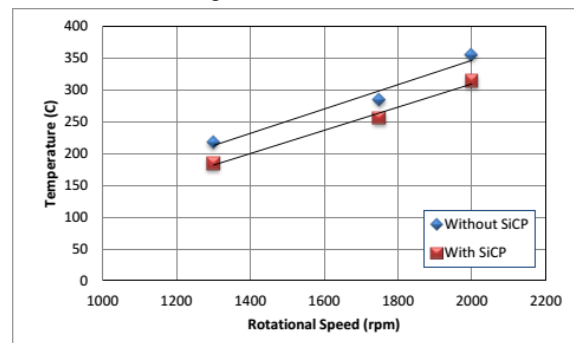


Fig. 14: Effects of rotational speeds on the friction temperature for joining pieces of 6061 aluminum alloy.

2. Conclusion

SiC_p was utilized in this study to improve the mechanical properties of the samples during FSW. The microstructure as well as mechanical parameters such as tensile strength, fracture surface, and microhardness were investigated. In the SZ, the 6061 aluminum alloy matrix containing SiC_p was created. Because of the effective stirring action of the pin and the desired heat input factor, the particle distribution was enhanced at 1750 rpm. By limiting recrystallized grain growth, recreating nucleation sites, and breaking initial particles during deformation, the SiC_p refined the microstructure. The sample friction stir-welded with SiC_p had a 37.2 percent higher UTS

at 1750 rpm than the sample friction stir-welded without SiCP reinforcement.

Acknowledgements

The Universiti Malaysia Perlis (UniMAP) provided funding for this study under grant number 9001-00338. The authors thank the employees of the Materials Engineering School (UniMAP), UTM Centre for Low Carbon Transport, Imperial College London, Universiti Teknologi Malaysia (UTM), and Universiti Sains Malaysia's School of Materials Engineering and Mineral Resources (USM).

References

- [1] K. Elangovan, V. Balasubramanian, Influences of tool pin profile and welding speed on the formation of friction stir processing zone in AA2219 aluminium alloy, *Journal of materials processing technology* 200(1) (2008) 163-175.
- [2] L. Ceschini, I. Boromei, G. Minak, A. Morri, F. Tarterini, Effect of friction stir welding on microstructure, tensile and fatigue properties of the AA7005/10vol.% Al₂O₃ composite, *Composites science and technology* 67(3) (2007) 605-615.
- [3] M. Ellis, Joining of aluminium based metal matrix composites, *International Materials Reviews* 41(2) (1996) 41-58.
- [4] K.N. Salloomi, Fully coupled thermomechanical simulation of friction stir welding of aluminum 6061-T6 alloy T-joint, *Journal of Manufacturing Processes* 45 (2019) 746-754.
- [5] L. Zhang, H. Zhong, S. Li, H. Zhao, J. Chen, L. Qi, Microstructure, mechanical properties and fatigue crack growth behavior of friction stir welded joint of 6061-T6 aluminum alloy, *International Journal of Fatigue* 135 (2020) 105556.
- [6] A. Kalinenko, K. Kim, I. Vysotskiy, I. Zuiko, S. Malopheyev, S. Mironov, R. Kaibyshev, Microstructure-strength relationship in friction-stir welded 6061-T6 aluminum alloy, *Materials Science and Engineering: A* 793 (2020) 139858.
- [7] R.S. Mishra, Z. Ma, Friction stir welding and processing, *Materials Science and Engineering: R: Reports* 50(1) (2005) 1-78.
- [8] J.-H. Cho, D.E. Boyce, P.R. Dawson, Modeling strain hardening and texture evolution in friction stir welding of stainless steel, *Materials Science and Engineering: A* 398(1) (2005) 146-163.
- [9] G.F. Liu, T.J. Chen, Z.J. Wang, Effects of solid solution treatment on microstructure and mechanical properties of SiCp/2024 Al composite: A comparison with 2024 Al alloy,

- Materials Science and Engineering: A* (2021) 141413.
- [10] A. Abdollahzadeh, A. Shokuhfar, J.M. Cabrera, A.P. Zhilyaev, H. Omidvar, In-situ nanocomposite in friction stir welding of 6061-T6 aluminum alloy to AZ31 magnesium alloy, *Journal of Materials Processing Technology* 263 (2019) 296-307.
- [11] H.J. Zhang, S.L. Sun, H.J. Liu, Z. Zhu, Y.L. Wang, Characteristic and mechanism of nugget performance evolution with rotation speed for high-rotation-speed friction stir welded 6061 aluminum alloy, *Journal of Manufacturing Processes* 60 (2020) 544-552.
- [12] Y. Helal, Z. Boumerzoug, L. Fellah, Microstructural evolution and mechanical properties of dissimilar friction stir lap welding aluminum alloy 6061-T6 to ultra low carbon steel, *Energy Procedia* 157 (2019) 208-215.
- [13] S. RaviKumar, R. KajaBanthaNavas, P. Sai Sujeeth, Multiple Response Optimization Studies for Dissimilar Friction Stir Welding Parameters of 6061 to 7075 Aluminium Alloys, *Materials Today: Proceedings* 16 (2019) 405-412.
- [14] S. Choudhary, S. Choudhary, S. Vaish, A.K. Upadhyay, A. Singla, Y. Singh, Effect of welding parameters on microstructure and mechanical properties of friction stir welded Al 6061 aluminum alloy joints, *Materials Today: Proceedings* 25 (2020) 563-569.
- [15] C. Rathinasuriyan, S. Muniamuthu, A. Mystica, V.S. Senthil Kumar, Investigation of heat generation during submerged friction stir welding on 6061-T6 aluminum alloy, *Materials Today: Proceedings* (2021).
- [16] S. Suresh, N. Elango, K. Venkatesan, W.H. Lim, K. Palanikumar, S. Rajesh, Sustainable friction stir spot welding of 6061-T6 aluminium alloy using improved non-dominated sorting teaching learning algorithm, *Journal of Materials Research and Technology* 9(5) (2020) 11650-11674.
- [17] T. Singh, S.K. Tiwari, D.K. Shukla, Effect of nano-sized particles on grain structure and mechanical behavior of friction stir welded Al-nanocomposites, *Proceedings of the Institution of Mechanical Engineers, Part L: Journal of Materials: Design and Applications* 234(2) (2019) 274-290.
- [18] Y. Kim, H. Fujii, T. Tsumura, T. Komazaki, K. Nakata, Three defect types in friction stir welding of aluminum die casting alloy, *Materials Science and Engineering: A* 415(1) (2006) 250-254.
- [19] H. Uzun, Friction stir welding of SiC particulate reinforced AA2124 aluminium alloy matrix

- composite, *Materials & design* 28(5) (2007) 1440-1446.
- [20] D. Storjohann, S. Babu, S. David, P. Sklad, Friction stir welding of aluminum metal matrix composites, *Proceeding of the 4th International Symposium On Friction Stir Welding*, Utah, 2003.
- [21] M. Barmouz, P. Asadi, M. Besharati Givi, M. Taherishargh, Investigation of mechanical properties of Cu/SiC composite fabricated by FSP: Effect of SiC particles' size and volume fraction, *Materials Science and Engineering: A* 528(3) (2011) 1740-1749.
- [22] S. Alidokht, A. Abdollah-Zadeh, S. Soleymani, H. Assadi, Microstructure and tribological performance of an aluminium alloy based hybrid composite produced by friction stir processing, *Materials & Design* 32(5) (2011) 2727-2733.
- [23] G. Faraji, P. Asadi, Characterization of AZ91/alumina nanocomposite produced by FSP, *Materials Science and Engineering: A* 528(6) (2011) 2431-2440.
- [24] A. Shamsipur, S.F. Kashani-Bozorg, A. Zarei-Hanzaki, The effects of friction-stir process parameters on the fabrication of Ti/SiC nanocomposite surface layer, *Surface and Coatings Technology* 206(6) (2011) 1372-1381.
- [25] M. Sharifitabar, A. Sarani, S. Khorshahian, M. Shafiee Afarani, Fabrication of 5052Al/Al₂O₃ nanoceramic particle reinforced composite via friction stir processing route, *Materials & Design* 32(8) (2011) 4164-4172.
- [26] M. Barmouz, M.K.B. Givi, Fabrication of in situ Cu/SiC composites using multi-pass friction stir processing: Evaluation of microstructural, porosity, mechanical and electrical behavior, *Composites Part A: Applied Science and Manufacturing* 42(10) (2011) 1445-1453.
- [27] M.B. Uday, M.N. Ahmad-Fauzi, Joint properties of friction welded 6061 aluminum alloy/YSZ-alumina composite at low rotational speed, *Materials & Design* 59 (2014) 76-83.
- [28] M. Barmouz, M.K. Besharati Givi, J. Seyfi, On the role of processing parameters in producing Cu/SiC metal matrix composites via friction stir processing: Investigating microstructure, microhardness, wear and tensile behavior, *Materials characterization* 62(1) (2011) 108-117.
- [29] A. Dolatkah, P. Golbabaie, M. Besharati Givi, F. Molaiekiya, Investigating effects of process parameters on microstructural and mechanical properties of Al5052/SiC metal matrix composite fabricated via friction stir processing, *Materials & Design* 37 (2012) 458-464.
- [30] M. Zohoor, M. Besharati Givi, P. Salami, Effect of processing parameters on fabrication of Al-Mg/Cu composites via friction stir processing, *Materials & Design* 39 (2012) 358-365.
- [31] Y. Sun, H. Fujii, The effect of SiC particles on the microstructure and mechanical properties of friction stir welded pure copper joints, *Materials Science and Engineering: A* 528(16) (2011) 5470-5475.
- [32] H.I. Dawood, K.S. Mohammed, A. Rahmat, M. Uday, The influence of the surface roughness on the microstructures and mechanical properties of 6061 aluminium alloy using friction stir welding, *Surface and Coatings Technology* 270 (2015) 272-283.
- [33] S.J. Bailey, N. Baldini, *Annual book of ASTM standards*, ASTM International, PA, USA (2007).
- [34] H. Khodaverdizadeh, A. Heidarzadeh, T. Saeid, Effect of tool pin profile on microstructure and mechanical properties of friction stir welded pure copper joints, *Materials & Design* 45 (2013) 265-270.
- [35] Y. Morisada, H. Fujii, T. Nagaoka, M. Fukusumi, Effect of friction stir processing with SiC particles on microstructure and hardness of AZ31, *Materials Science and Engineering: A* 433(1) (2006) 50-54.
- [36] Y. Morisada, H. Fujii, T. Nagaoka, M. Fukusumi, MWCNTs/AZ31 surface composites fabricated by friction stir processing, *Materials Science and Engineering: A* 419(1) (2006) 344-348.
- [37] M.M. El-Rayes, E.A. El-Danaf, The influence of multi-pass friction stir processing on the microstructural and mechanical properties of Aluminum Alloy 6082, *Journal of Materials Processing Technology* 212(5) (2012) 1157-1168.
- [38] A. Rollett, F. Humphreys, G.S. Rohrer, M. Hatherly, *Recrystallization and related annealing phenomena*, Elsevier 2004.
- [39] M.B. Uday, M.N. Ahmad Fauzi, H. Zuhailawati, A.B. Ismail, Thermal analysis of friction welding process in relation to the welding of YSZ-alumina composite and 6061 aluminum alloy, *Applied Surface Science* 258(20) (2012) 8264-8272.
- [40] A. Feng, B. Xiao, Z. Ma, Effect of microstructural evolution on mechanical properties of friction stir welded AA2009/SiCp composite, *Composites Science and Technology* 68(9) (2008) 2141-2148.
- [41] Y. Morisada, H. Fujii, T. Nagaoka, K. Nogi, M. Fukusumi, Fullerene/A5083 composites fabricated by material flow during friction stir processing, *Composites Part A: Applied Science and Manufacturing* 38(10) (2007) 2097-2101.

- [42] M. Bahrami, K. Dehghani, M.K.B. Givi, A novel approach to develop aluminum matrix nano-composite employing friction stir welding technique, *Materials & Design* 53 (2014) 217-225.
- [43] H. Nami, H. Adgi, M. Sharifitabar, H. Shamabadi, Microstructure and mechanical properties of friction stir welded Al/Mg₂ Si metal matrix cast composite, *Materials & Design* 32(2) (2011) 976-983.